meso-DNAs with Homopurine Sequences: Analysis of Their Interaction with Natural DNAs

Naoko IWANAMI,[a] Yuichi HASHIMOTO,*[,b] and Koichi SHUDO[a]

Faculty of Pharmaceutical Sciences, The University of Tokyo,[a] 7–3–1 Hongo, Bunkyo-ku, Tokyo 113, Japan and Institute of Molecular and Cellular Biosciences, The University of Tokyo,[b] 1–1–1 Yayoi, Bunkyo-ku, Tokyo 113, Japan.
Received November 20, 1995; accepted December 29, 1995

Two homopurine sequences of *meso*-DNAs (DNAs having an alternating sequence of 2-deoxy-L-ribose and 2-deoxy-D-ribose in their sugar moieties), d(LADG)$_5$ and d(LGDA)$_5$, were prepared. Both d(LADG)$_5$ and d(LGDA)$_5$ interacted with the corresponding complementary natural DNAs, d(DCDT)$_5$ and d(DTDC)$_5$, respectively. In the interactions, pH-dependent duplex/triplex selectivity was observed, *i.e.*, *meso*-d(Pu)$_{10}$ formed a duplex at pH 7.5 and a triplex at pH 5.0 with the complementary D-d(Py)$_{10}$. The *meso*-d(Pu)$_{10}$/D-d(Py)$_{10}$ complex showed a CD spectrum similar in shape to that of the natural complex, suggesting that *meso*/natural complexes form right-handed helices. At pH 7.5, ethidium bromide intercalated into both d(LADG)$_5$/d(DCDT)$_5$ and d(LGDA)$_5$/d(DTDC)$_5$ duplexes. A clear difference between d(LADG)$_5$/d(DCDT)$_5$ and d(LGDA)$_5$/d(DTDC)$_5$ was observed at pH 5.0. Addition of ethidium bromide did not affect the formed d(LADG)$_5$/d(DCDT)$_5$ triplex, and ethidium bromide did not intercalate into the triplex. On the other hand, d(LGDA)$_5$ did not form a triplex with d(DTDC)$_5$ in the presence of ethidium bromide even at pH 5.0, but it formed a duplex. Ethidium bromide intercalated into the duplex at pH 5.0.

Key words *meso*-DNA; interaction; duplex/triplex selectivity; intercalation

In natural nucleic acids, the higher-order structure is mainly determined by the chirality of the sugar–backbone units. Organisms in our world utilize only D-sugars, but not their enantiomers, probably for reasons closely related to the origin and the evolution of life. Nevertheless, molecular modeling studies suggest that an L-sugar backbone can locate nucleobases appropriately for complementary base-pairing with natural nucleic acids by Watson–Crick or Hoogsteen base-pairing.[1-6] This raises the possibility that L-sugar-containing nucleic acids might function as pseudo-DNA/pseudo-RNA.[1,4-18]

Huge numbers of nucleic acid derivatives and analogs have been synthesized.[19-24] L-Sugar-containing nucleic acids [*enantio*-DNA (DNA having 2-deoxy-L-*erythro*-pentose, the enantiomer of natural 2-deoxy-D-ribose, in the backbone) and *meso*-DNA (DNA having an alternating sequence of L-sugar and D-sugar)] offer a simple approach to the molecular design of pseudo-DNA (Fig. 1). It was anticipated that they would act as antisense/antigene oligonucleotides. In addition, as enzymes generally recognize only naturally occurring stereoisomers, it is expected that *enantio*/*meso*-DNA would not be a substrate for nucleases, whose oligonucleotide-degrading activity imposes a severe restriction upon antisense/antigene strategies.[19-24]

Recently, we have reported the preparation of a dodecamer of *enantio*-deoxyadenylic acid [L-(dAp)$_{11}$dA, designated as L-dA$_{12}$] and its interaction with the complementary polymers, poly(U) (RNA-type) and poly(dT) (DNA-type).[1,7-9] L-dA$_{12}$ was quite resistant to nucleases. It showed affinity for both poly(U) and poly(dT), and the measured melting temperature (T_m) values showed

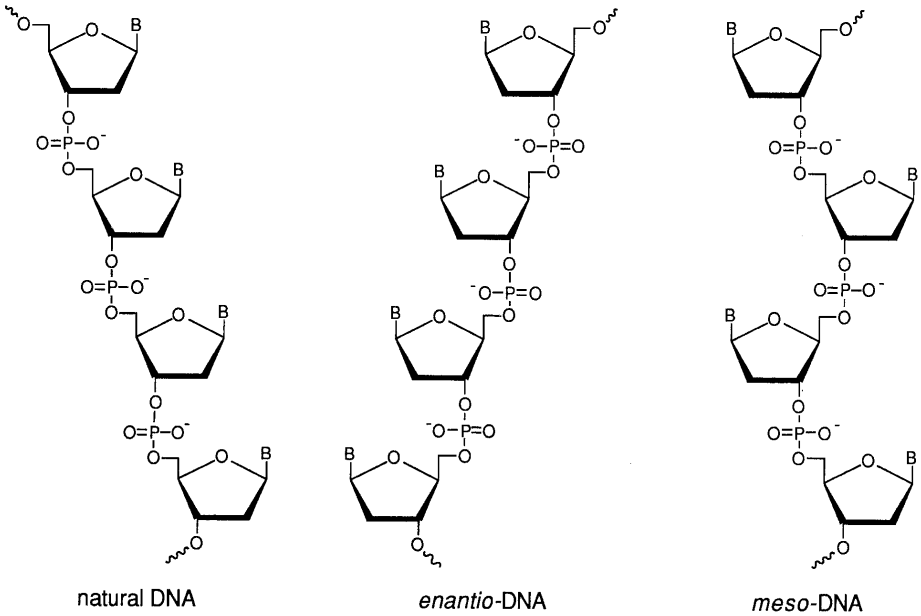

Fig. 1. *enantio*-DNA and *meso*-DNA

* To whom correspondence should be addressed.

high selectivity of L-dA_{12} for poly(U) over poly(dT). L-dA_{12} did not show any hypochromicity when mixed with poly(G), poly(A), or poly(C), indicating that the triplex formation is complementary base-specific. The mode of interaction of L-dA_{12} with poly(U) or poly(dT) was suggested to be triplex formation, on the bases of both UV-mixing curve experiments[1] and *ab initio* calculation for molecular modeling study.[2] In addition, we prepared *enantio*-DNAs bearing nucleobases other than adenine, and reported their interaction with natural nucleic acids. We also reported the preparation of *meso*-DNA [(L-dA·D-dA)$_6$, designated as LD-dA_{12}] and its interaction with the complementary natural nucleic acids.[8-11] LD-dA_{12} showed intermediate characteristics between D-dA_{12} and L-dA_{12} as regards its interaction with natural nucleic acids, and it had adequate stability to nucleases. *meso*-DNA should be more useful for antisense/antigene strategies, because of its formation of stable complexes with the complementary natural nucleic acids and its sufficient stability to nucleases. As a continuation of our earlier investigation on *meso*-DNAs, we designed *meso*-DNA oligomers having homopurine sequences, *i.e.*, (L-dA·D-dG)$_5$ and (L-dG·D-dA)$_5$, designated as d(LAdG)$_5$ and d(LGdA)$_5$, respectively. In this paper, we describe the interaction of these *meso*-DNAs with complementary natural DNA, their selective pH-dependent duplex/triplex formation with natural DNAs, and the intercalation of ethidium bromide into *meso*/natural DNA complexes.

Experimental

Preparation of *meso*-DNAs L-Deoxynucleotide-cyanoethyl phosphoramidites were synthesized as described previously.[9,25-29] Acetonitrile solutions of synthesized L-dN-amidites and commercially available D-dN-amidites were used in a DNA-Synthesizer Model 391 PCR-MATE equipped with a commercially available CPG-column (Applied Biosystems Inc.). The complementary natural DNAs, d(DCdT)$_5$ and d(DTdC)$_5$, were synthesized similarly. Oligomers containing L-dN were synthesized according to the instructions supplied with the machine. The synthesized oligomers were purified by HPLC using a Polygosil 60-5 C_{18} column (0.8 cm o.d. × 25 cm) eluted with 0.05 M triethylammonium acetate pH 7.0 buffer containing 8—20% acetonitrile, then desalted by flash column chromatography using a silica gel ODS-Q3 column (1.8 cm o.d. × 15 cm) eluted with water containing 0—20% acetonitrile or by using a NAP 25 column (Pharmacia). Quantification of the obtained oligonucleotides was performed by measuring UV absorption at 260 nm (A_{260}) and employing extinction coefficients of 9500 and 7500 l mol^{-1} cm^{-1} for d(Pu)$_{10}$ and d(Py)$_{10}$, respectively.[30]

UV-Mixing Curves A solution of synthesized *meso*-d(Pu)$_{10}$ [0.09 mM nucleotide-units (0.09 mM (n.u.)) in 10 mM Tris–HCl (pH 7.5) containing 10 mM $MgCl_2$ (TM buffer pH 7.5) or in 20 mM sodium acetate (pH 5.0) containing 10 mM $MgCl_2$ (AM buffer pH 5.0)] and a solution of complementary D-d(Py)$_{10}$ (0.09 mM (n.u.) in the same buffer) were mixed in various ratios. The mixtures were heated to 80 °C for 5 min, then slowly cooled to room temperature, and subsequently cooled to 4 °C overnight. The UV absorption spectra were measured by a UV/VIS spectrophotometer (V-550, JASCO) equipped with a temperature controller (ETC-505, JASCO). The absorption ratios at the wavelength of the isosbestic point for *meso*-d(Pu)$_{10}$ and D-d(Py)$_{10}$ were plotted. In each case, the optical density of a 0.09 mM (n.u.) solution of *meso*-d(Pu)$_{10}$ oligomer was assigned the value of 1.0.

Circular Dichroism (CD) Spectra Mixture solutions of 0.03 mM (n.u.) *meso*-d(Pu)$_{10}$ and D-d(Py)$_{10}$ (1:0, 1:1, 1:2, 0:1) in TM buffer pH 7.5 or AM buffer pH 5.0 were prepared, then heated and cooled as described above. The CD spectra of the samples were measured by using a spectropolarimeter (J-600, JASCO) equipped with a thermocontroller (TRL-108H, Tomasz Ltd.).

Melting-Temperature Measurement Solutions of 0.09 mM (n.u.) *meso*-d(Pu)$_{10}$ and of D-d(Py)$_{10}$ were mixed in the molar nucleotide-units ratio of 1:1 in TM buffer pH 7.5 or 1:2 in AM buffer pH 5.0. Each mixture was heated and cooled as described above. The temperature of each mixture solution was gradually increased (0.5 °C per minute) and UV absorption at 260 nm was monitored by a UV/VIS spectrophotometer (V-550, JASCO) equipped with a temperature controller (ETC-505, JASCO). Melting temperatures, T_m, were calculated from the maximum in the first derivative plot.

Ethidium Bromide Intercalation Study An excess (final 0.04 mM) of ethidium bromide was added to the same sample as that used in the CD-spectral measurement. The sample was heated and incubated as described above. For fluorescence measurement, the excitation wavelength was set at 546 nm. Emission spectra (560—660 nm) were measured by a spectrofluorometer (FP-770F, JASCO) equipped with a thermocontroller (TRL-108H, Tomasz Ltd.). Mixing curves and melting temperatures in the presence of ethidium bromide were measured as described above, except that the mixture contained an excess (final 0.04 mM) of ethidium bromide.

Fluorescence Study for Scatchard Analysis Solutions of *meso*-d(Pu)$_{10}$ and D-d(Py)$_{10}$ were mixed at 1:1 stoichiometry in TM buffer pH 7.5, and used for titration of ethidium bromide. The samples contained from 0 to 120 μM (n.u) DNA and 0.3 μM ethidium bromide. The mixtures were heated and cooled as described above, except that they were cooled to −8 °C, and the fluorescence was measured at −8 °C to obtain results with superior reproducibility (freezing did not occur at that temperature). For fluorescence measurement, the excitation wavelength was set at 505 nm. Emission spectra (530—700 nm) were measured by a spectrofluorometer (FP-770F, JASCO). Fluorescence enhancement was evaluated from the area under the emission curve.

Results

Interaction of *meso*-d(Pu)$_{10}$ with Natural D-d(Py)$_{10}$ and pH-Dependent Duplex/Triplex Selectivity To investigate the interaction of *meso*-d(Pu)$_{10}$ with natural D-d(Py)$_{10}$, we initially measured UV-mixing curves by the method of continuous variations (Fig. 2). In TM buffer pH 7.5 at 0 °C, the d(LAdG)$_5$/d(DCdT)$_5$ and d(LGdA)$_5$/d(DTdC)$_5$ mixing curves showed the maximum hypochromicity, 19% and 13% respectively, at d(Py)$_{10}$ = 50%, *i.e.*, Pu:Py = 1:1 molar ratio. The result indicates that the interaction of *meso*-d(Pu)$_{10}$ with D-d(Py)$_{10}$ is duplex formation under the experimental conditions used. The hypochromicity disappeared and the mixing curves became linear at 20 °C, indicating that the T_m values of *meso*-d(Pu)$_{10}$/D-d(Py)$_{10}$ duplexes were between 0 °C and 20 °C. On the other hand, in AM buffer pH 5.0, the maximum hypochromicity appeared at the point d(Py)$_{10}$ = 65%, *i.e.*, Pu:Py = 1:2 molar ratio, indicating that *meso*-d(Pu)$_{10}$/D-d(Py)$_{10}$ forms a triplex at pH 5.0, while it forms a duplex at pH 7.5 (*vide supra*). The values of maximum hypochromicity observed for d(LAdG)$_5$/d(DCdT)$_5$ and d(LGdA)$_5$/d(DTdC)$_5$ at pH 5.0 were 20% and 17%, respectively. These hypochromicities could also be observed at 20 °C, but disappeared at 40 °C. It is noteworthy that the duplex/triplex selectivity is dependent on pH. Similar pH-dependent duplex/triplex selectivity was observed in the interaction of the corresponding natural isomer, D-d(Pu)$_{10}$/D-d(Py)$_{10}$ (data not shown).

These interactions were also confirmed by observation of the CD spectra. When an oligomer forms a complex with its complementary oligomer, the CD spectrum deviates from the simulated mean of the separate spectra of the two oligomers (summation of spectra of an oligomer and of its complementary oligomer). Such a phenomenon was observed when *meso*-d(Pu)$_{10}$ was mixed with D-d(Py)$_{10}$ at a temperature lower than the T_m value.

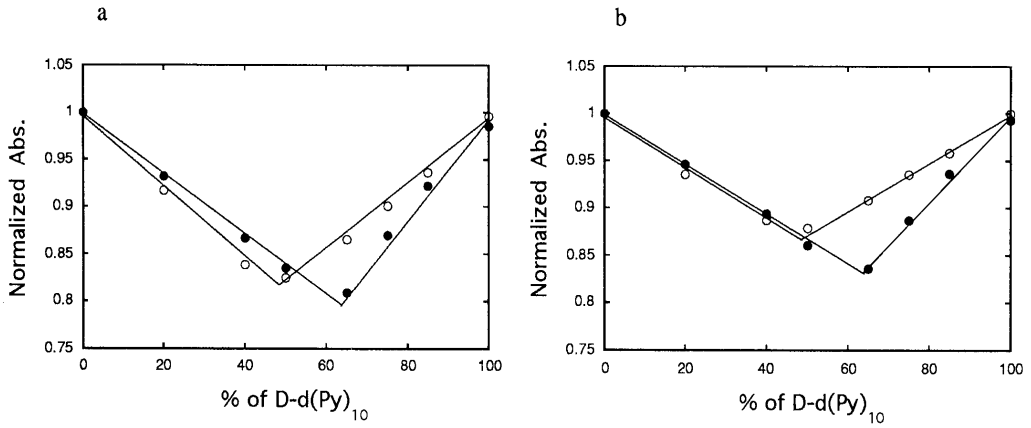

Fig. 2. UV-Mixing Curves

(a) d(LAdG)$_5$ mixed with d(DCdT)$_5$ and (b) d(LGdA)$_5$ mixed with d(DTdC)$_5$ at 0 °C. —○—, in TM buffer pH 7.5 (10 mM Tris–HCl, 10 mM $MgCl_2$); —●—, in AM buffer pH 5.0 (20 mM sodium acetate, 10 mM $MgCl_2$).

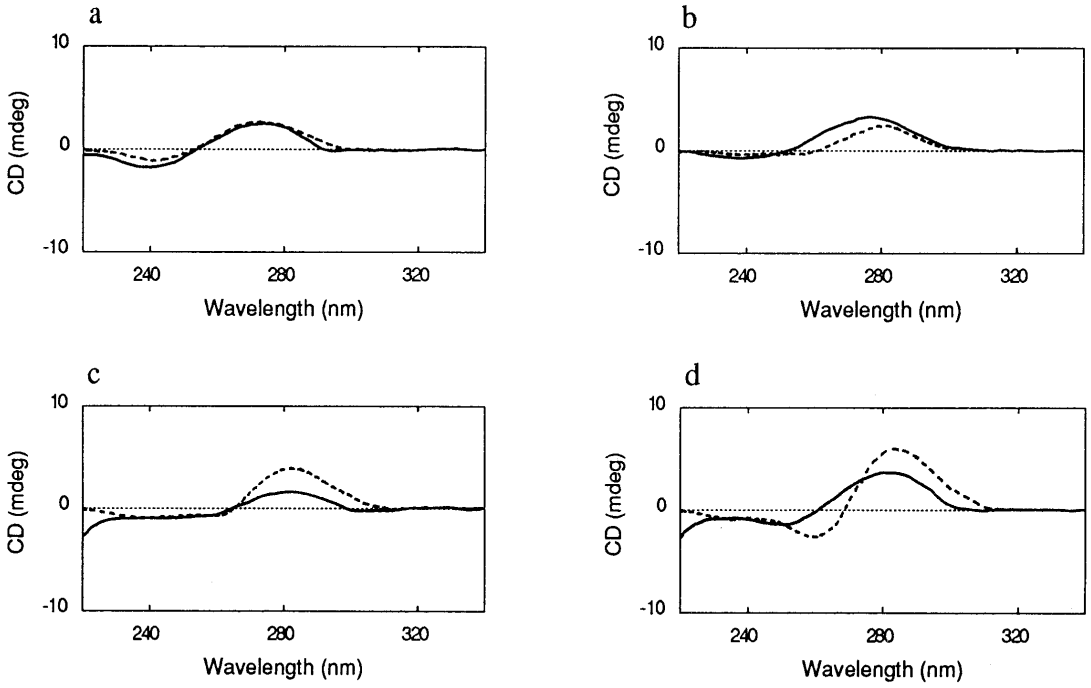

Fig. 3. Comparison between Observed and Simulated CD Spectra

(a) Mixture of d(LAdG)$_5$ and d(DCdT)$_5$ (1 : 1) at pH 7.5, 0 °C. (b) Mixture of d(LGdA)$_5$ and d(DTdC)$_5$ (1 : 1) at pH 7.5, 0 °C. (c) Mixture of d(LAdG)$_5$ and d(DCdT)$_5$ (1 : 2) at pH 5.0, 0 °C. (d) Mixture of d(LGdA)$_5$ and d(DTdC)$_5$ (1 : 2) at pH 5.0, 0 °C. ——, observed spectrum; ------, simulated spectrum.

Figure 3 shows a comparison of the simulated and the observed CD spectra of *meso*-d(Pu)$_{10}$/D-d(Py)$_{10}$ mixtures at 0 °C. In all cases shown in the figure, a deviation of the observed from the simulated spectra was apparent. A blue shift was observed for the 1 : 1 mixture at pH 7.5, and a diminution of the peak at 280 nm was observed for the 1 : 2 mixture at pH 5.0. These deviations disappeared at higher temperature, 20 °C for the 1 : 1 and 40 °C for the 1 : 2 mixture, leaving a spectrum identical with the simulated form. It is possible to discriminate duplex formation from triplex formation by comparison of the measured CD spectrum with the simulated spectrum. For example, at pH 7.5, the observed spectrum of a mixture containing *meso*-d(Pu)$_{10}$ and D-d(Py)$_{10}$ in 1 : 2 molar ratio was identical with the spectrum simulated on the basis that the mixture contains 2 volumes of meso : natural = 1 : 1 mixture and 1 volume of D-d(Py)$_{10}$ solution. On the other hand, the observed spectrum of a mixture containing *meso*-d(Pu)$_{10}$ and D-d(Py)$_{10}$ in 1 : 1 molar ratio (Fig. 3a, 3b) was not identical with a spectrum simulated on the basis that it contains 3 volumes of meso : natural = 1 : 2 mixture and 1 volume of *meso*-d(Pu)$_{10}$ solution. These results showed that duplex and single strand exist in TM buffer pH 7.5. The results at pH 5.0 indicated that triplex and single strand exist in AM buffer pH 5.0. CD spectra also give information about the conformations of the complexes. A comparison of the CD spectra of *meso*-d(Pu)$_{10}$/D-d(Py)$_{10}$ complexes with those of the corresponding natural complexes is shown in Fig. 4. CD spectra of the *meso*-d(Pu)$_{10}$/D-d(Py)$_{10}$ complexes are similar in shape to those of the corresponding natural right-handed complexes. This similarity suggests that *meso*-d(Pu)$_{10}$/D-d(Py)$_{10}$ complex also possesses right-handed conformation.

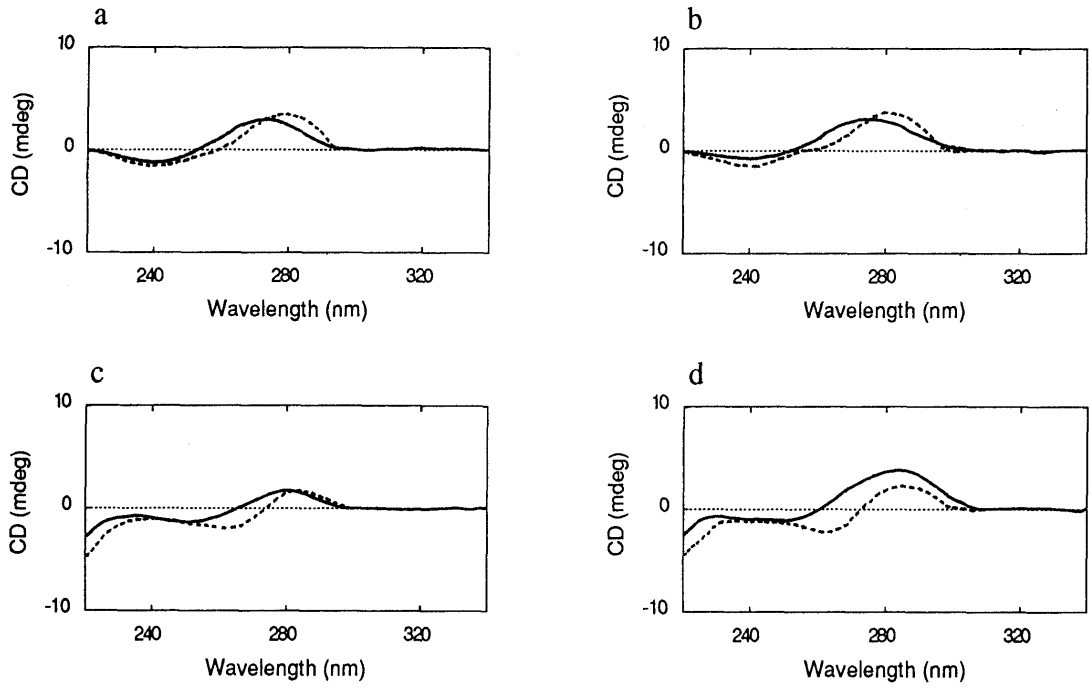

Fig. 4. Comparison of CD Spectra between *meso*/Natural and the Corresponding Natural Complexes

(a) Duplex of $d(AG)_5/d(CT)_5$ at pH 7.5, 0 °C. ——, $d(\text{L}A\text{D}G)_5/d(\text{D}C\text{D}T)_5$ ------; $d(\text{D}A\text{D}G)_5/d(\text{D}C\text{D}T)_5$. (b) Duplex of $d(GA)_5/d(TC)_5$ at pH 7.5, 0 °C. ——, $d(\text{L}G\text{D}A)_5/d(\text{D}T\text{D}C)_5$. ------, $d(\text{D}G\text{D}A)_5/d(\text{D}T\text{D}C)_5$. (c) Triplex of $d(AG)_5/2d(CT)_5$ at pH 5.0, 0 °C. ——, $d(\text{L}A\text{D}G)_5/2d(\text{D}C\text{D}T)_5$; ------; $d(\text{D}A\text{D}G)_5/2d(\text{D}C\text{D}T)_5$. (d) Triplex of $d(GA)_5/2d(TC)_5$ at pH 5.0, 0 °C. ——; $d(\text{L}G\text{D}A)_5/2d(\text{D}T\text{D}C)_5$; ------, $d(\text{D}G\text{D}A)_5/2d(\text{D}T\text{D}C)_5$.

Stability of *meso*-d(Pu)$_{10}$/D-d(Py)$_{10}$ Complex T_m profiles for complexes of *meso*-$d(Pu)_{10}$ with D-$d(Py)_{10}$ were investigated (Fig. 5). All melting curves of *meso*-$d(Pu)_{10}$/D-$d(Py)_{10}$ complexes showed monophasic transition profiles. The T_m value of the $d(\text{L}A\text{D}G)_5/d(\text{D}C\text{D}T)_5$ duplex at pH 7.5 was 12 °C, while T_m of the natural duplex $d(\text{D}A\text{D}G)_5/d(\text{D}C\text{D}T)_5$ was 40 °C; and the T_m of the $d(\text{L}G\text{D}A)_5/d(\text{D}T\text{D}C)_5$ duplex at pH 7.5 was 10 °C, while the T_m of the natural duplex $d(\text{D}G\text{D}A)_5/d(\text{D}T\text{D}C)_5$ was 39 °C. The T_m of $d(\text{L}A\text{D}G)_5/2d(\text{D}C\text{D}T)_5$ triplex at pH 5.0 was 34 °C, while T_m of the natural triplex $d(\text{D}A\text{D}G)_5/2d(\text{D}C\text{D}T)_5$ was 45 °C; and T_m of the $d(\text{L}G\text{D}A)_5/2d(\text{D}T\text{D}C)_5$ triplex at pH 5.0 was 24 °C, while T_m of the natural triplex $d(\text{D}G\text{D}A)_5/2d(\text{D}T\text{D}C)_5$ was 42 °C. The results suggest that the *meso*-$d(Pu)_{10}$/D-$d(Py)_{10}$ complex is less stable than the corresponding natural complex. It is also indicated that the $d(\text{L}A\text{D}G)_5/d(\text{D}C\text{D}T)_5$ complex is more stable than the $d(\text{L}G\text{D}A)_5/d(\text{D}T\text{D}C)_5$ complex, and the difference becomes greater when they form a triplex at pH 5.0.

Ethidium Bromide Intercalation Study The intercalation activity of ethidium bromide into *meso*-$d(Pu)_{10}$/D-$d(Py)_{10}$ complexes was investigated (Fig. 6). A single strand or a mixture of *meso*-$d(Pu)_{10}$ and D-$d(Py)_{10}$ (in all samples, the concentration of the total nucleic acids was adjusted to be 0.03 mM (n.u.)) was added to excess (0.04 mM) ethidium bromide solution. Addition of single-stranded *meso*-$d(Pu)_{10}$ or D-$d(Py)_{10}$ did not increase the ethidium fluorescence in TM buffer pH 7.5 or AM buffer pH 5.0, though addition of the $d(\text{L}A\text{D}G)_5/d(\text{D}C\text{D}T)_5$ or $d(\text{L}G\text{D}A)_5/d(\text{D}T\text{D}C)_5$ mixture caused a clear enhancement of fluorescence intensity at pH 7.5. The enhancement of the fluorescence suggests intercalation of ethidium at a hydrophobic site of the *meso*-$d(Pu)_{10}$/D-$d(Py)_{10}$ duplex.

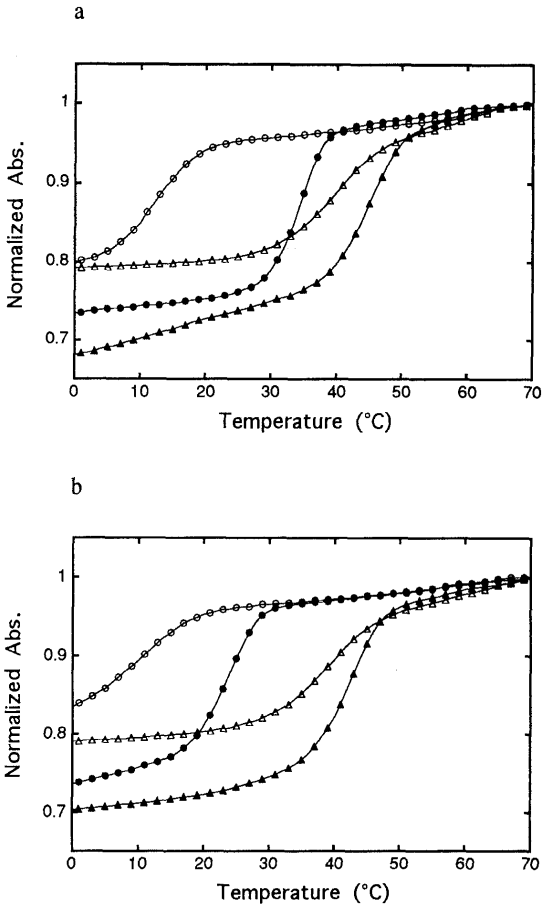

Fig. 5. Melting Temperature Profiles

(a) $d(\text{L}A\text{D}G)_5/d(\text{D}C\text{D}T)_5$ and the corresponding natural complex. (b) $d(\text{L}G\text{D}A)_5/d(\text{D}T\text{D}C)_5$ and the corresponding natural complex. —○—, mixture of *meso*-$d(Pu)_{10}$ and D-$d(Py)_{10}$ (1 : 1) at pH 7.5. —●—, mixture of *meso*-$d(Pu)_{10}$ and D-$d(Py)_{10}$ (1 : 2) at pH 5.0. —△—, mixture of natural D-$d(Pu)_{10}$ and D-$d(Py)_{10}$ (1 : 1) at pH 7.5. —▲—, mixture of natural D-$d(Pu)_{10}$ and D-$d(Py)_{10}$ (1 : 2) at pH 5.0.

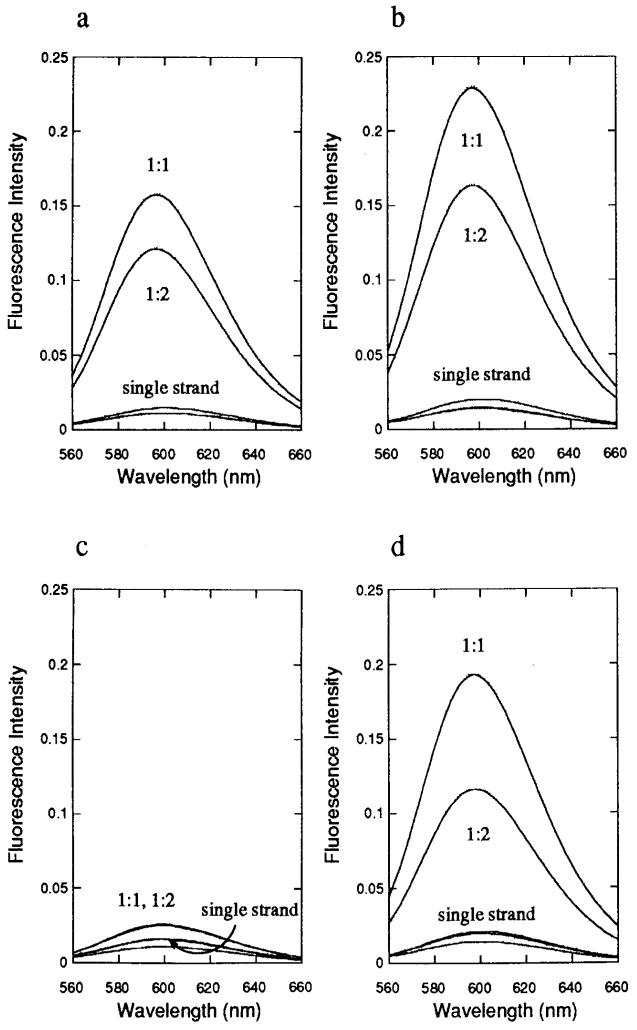

Fig. 6. Fluorescence Spectra of Ethidium Bromide with DNAs

(a) Mixture or single strand of d(LAdG)$_5$ and d(dTdC)$_5$ at pH 7.5, 0 °C. (b) Mixture or single strand of d(LGdA)$_5$ and d(dCdT)$_5$ at pH 7.5, 0 °C. (c) Mixture or single strand of d(LAdG)$_5$ and d(dTdC)$_5$ at pH 5.0, 0 °C. (d) Mixture or single strand of d(LGdA)$_5$ and d(dTdC)$_5$ at pH 5.0, 0 °C.

The enhancement was observed at 0 °C and 20 °C, but not at 40 °C, indicating that the T_m values are between 20 °C and 40 °C. Similar enhancement of ethidium fluorescence was observed upon addition of d(LGdA)$_5$/d(dTdC)$_5$ mixture at pH 5.0. However, addition of d(LAdG)$_5$/d(dCdT)$_5$ to the AM buffer pH 5.0 did not enhance the fluorescence. Therefore, the efficiency of the enhancement by 1 : 1 mixture was higher than that by 1 : 2, and that by d(LGdA)$_5$/d(dTdC)$_5$ mixture was higher than that by d(LAdG)$_5$/d(dCdT)$_5$ under the same conditions. Moreover, a blue shift of the emission spectrum upon addition of the duplex was observed. The peak of the emission spectrum of free ethidium appeared at 605 nm, and it shifted to 595 nm after the addition of *meso*-d(Pu)$_{10}$/D-d(Py)$_{10}$ duplex. A similar blue shift was observed upon addition of the corresponding natural duplex. These results suggest a similarity of the environment of the intercalation site between *meso*-d(Pu)$_{10}$/D-d(Py)$_{10}$ and the natural duplex. At pH 5.0, a difference in efficiency of enhancement was observed between d(LAdG)$_5$/d(dCdT)$_5$ and d(LGdA)$_5$/d(dTdC)$_5$. This was the first case where obviously different behavior between d(LAdG)$_5$ and d(LGdA)$_5$ was observed. In the case of d(LGdA)$_5$/d(dTdC)$_5$ at pH 5.0, a 1 : 1 mixture of d(LGdA)$_5$/d(dTdC)$_5$ gave a greater enhancement of ethidium fluorescence than a 1 : 2 mixture did, although it formed a triplex in the absence of ethidium. The superior efficiency of the enhancement for the 1 : 1 mixture over the 1 : 2 mixture suggests that (i) ethidium intercalated only into the duplex but not the triplex, or (ii) intercalation into the duplex causes higher enhancement than that into the triplex.

To investigate the mode of interaction between *meso*-d(Pu)$_{10}$ and D-d(Py)$_{10}$ in the presence of ethidium bromide, mixing curves in the presence of excess ethidium bromide were measured (Fig. 7). In ethidium bromide-containing TM buffer pH 7.5, a *meso*-d(Pu)$_{10}$/D-d(Py)$_{10}$ mixture showed maximum hypochromicity (30—35%) at the molar ratio of Pu : Py = 1 : 1. This indicates that both d(LAdG)$_5$/d(dCdT)$_5$ and d(LGdA)$_5$/d(dTdC)$_5$ formed duplexes even when they were intercalated by ethidium. A d(LAdG)$_5$/d(dCdT)$_5$ mixture, which did not increase the ethidium fluorescence at pH 5.0, showed maximum hypochromicity (20%) at the molar ratio of Pu : Py = 1 : 2, indicating that it formed a triplex even in the presence of ethidium bromide. On the other hand, a d(LGdA)$_5$/d(dTdC)$_5$ mixture, which enhanced the ethidium fluorescence intensity, showed maximum hypochromicity (35%) at the molar ratio of Pu : Py = 1 : 1, indicating that it formed a duplex in the presence of ethidium bromide, while the same mixture in the absence of ethidium bromide showed the maximum hypochromicity at the molar ratio of Pu : Py = 1 : 2 (*vide supra*). These results suggest that the mode of interaction of d(LGdA)$_5$ with d(dTdC)$_5$ at pH 5.0 is triplex formation in the absence of ethidium bromide, but changes to duplex formation in the presence of ethidium bromide.

Melting Temperature in the Presence of Ethidium Bromide The melting temperature of *meso*-d(Pu)$_{10}$/D-d(Py)$_{10}$ complexes in the presence or absence of excess ethidium bromide was investigated (Table 1). The concentration of DNA was standardized to 0.03 mM (n.u.) and the concentration of ethidium bromide was 0.04 mM. At pH 7.5, the T_m value of d(LAdG)$_5$/d(dCdT)$_5$ duplex was 22 °C in the presence of ethidium bromide, while it was 11 °C in the absence of ethidium bromide; and that of d(LGdA)$_5$/d(dTdC)$_5$ duplex was 27 °C in the presence of ethidium bromide, while it was 6 °C in the absence of ethidium bromide. At pH 7.5, ethidium bromide stabilized *meso*-d(Pu)$_{10}$/D-d(Py)$_{10}$ duplexes. The stabilizing effect was greater on d(LGdA)$_5$/d(dTdC)$_5$ (ΔT_m = 21 °C) than on d(LAdG)$_5$/d(dCdT)$_5$ (ΔT_m = 11 °C). At pH 5.0, the T_m value of d(LAdG)$_5$/d(dCdT)$_5$ triplex was 32 °C in the presence of ethidium bromide, while it was 36 °C in the absence of ethidium bromide. The d(LGdA)$_5$/d(dTdC)$_5$ duplex intercalated with ethidium bromide showed a T_m of 24 °C, and its triplex in the absence of ethidium bromide showed a T_m of 21 °C. The d(LAdG)$_5$/d(dCdT)$_5$ triplex seemed not to bind ethidium bromide at pH 5.0 (*vide infra*), and the T_m value of the triplex was little lower in the presence of ethidium bromide. The d(LAdG)$_5$/d(dCdT)$_5$ duplex intercalated by ethidium (T_m = 22 °C) is less stable than the triplex (T_m = 36 °C). This may be the reason why no conversion of the d(LAdG)$_5$/d(dCdT)$_5$ triplex to the duplex occurred upon addition of ethidi-

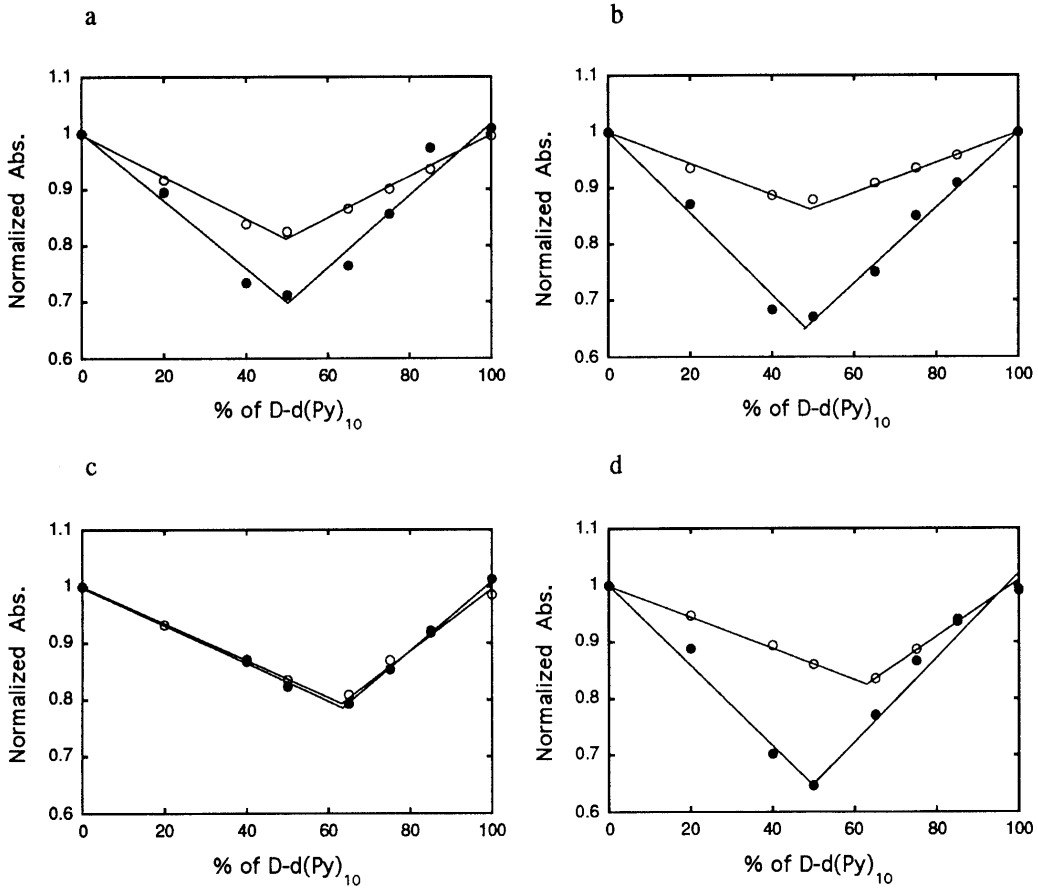

Fig. 7. Mixing Curves in the Presence or Absence of Ethidium Bromide

(a) d(LAdG)$_5$ mixed with d(DCdT)$_5$ at pH 7.5, 0 °C. (b) d(LGdA)$_5$ mixed with d(DTdC)$_5$ at pH 7.5, 0 °C. (c) d(LAdG)$_5$ mixed with d(DCdT)$_5$ at pH 5.0, 0 °C. (d) d(LGdA)$_5$ mixed with d(DTdC)$_5$ at pH 5.0, 0 °C; —○—, absence of ethidium bromide; —●—, presence of ethidium bromide.

Table 1. Effect of Ethidium Bromide on T_m Values and Duplex/Triplex Selectivities

		pH 7.5		pH 5.0	
d(LAdG)$_5$/d(DCdT)$_5$	−EtBr	11 °C	Duplex	36 °C	Triplex
	+EtBr	22 °C	Intercalated duplex	32 °C	Triplex
d(LGdA)$_5$/d(DTdC)$_5$	−EtBr	6 °C	Duplex	21 °C	Triplex
	+EtBr	27 °C	Intercalated duplex	24 °C	Intercalated duplex
d(DAdG)$_5$/d(DCdT)$_5$	−EtBr	38 °C	Duplex	46 °C	Triplex
	+EtBr	45 °C	Intercalated duplex	45 °C	Intercalated complex[a)]
d(DGdA)$_5$/d(DTdC)$_5$	−EtBr	37 °C	Duplex	40 °C	Triplex
	+EtBr	43 °C	Intercalated duplex	41 °C	Intercalated complex[a)]

The samples contain 0.03 mM (n.u.) DNA and 0.04 mM ethidium bromide. *a*) The natural complexes in AM buffer pH 5.0 containing EtBr are a mixture of duplex and triplex.

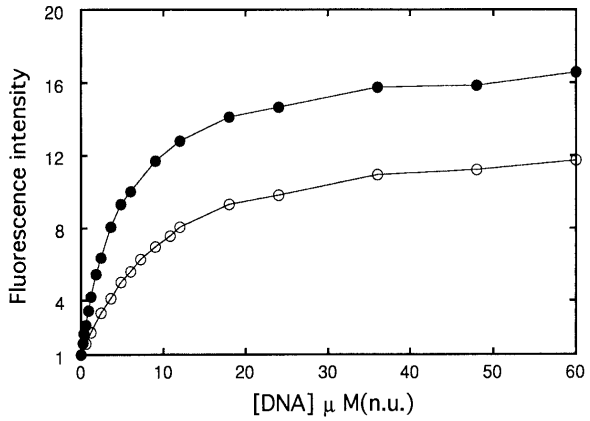

Fig. 8. Enhancement of Ethidium Fluorescence by Duplex Addition

—○—, duplex of d(LAdG)$_5$/d(DCdT)$_5$; —●—, duplex of d(LGdA)$_5$/d(DTdC)$_5$.

um bromide. In contrast, ethidium-bound d(LGdA)$_5$/d(DTdC)$_5$ duplex (T_m=24 °C at pH 5.0) is more stable than the corresponding triplex (T_m=21 °C). Though the difference in T_m is not great (ΔT_m=3 °C), it should be enough to allow conversion of the triplex into the ethidium bromide-intercalated duplex to occur in the case of d(LGdA)$_5$/d(DTdC)$_5$.

Fluorescence Titration Study and Scatchard Analysis To obtain information about the intercalation, Scatchard analysis was performed. Figure 8 shows the titration profiles of the fluorescence intensity of ethidium by *meso*-d(Pu)$_{10}$/D-d(Py)$_{10}$ 1 : 1 mixture in TM buffer pH 7.5. The value of fluorescence intensity was normalized based on the point of C_{DNA}=0, which was assigned the value 1.0. The intensity of ethidium fluorescence was enhanced by duplex addition and reached the maximum value of 13 with d(LAdG)$_5$/d(DCdT)$_5$, and 17 with d(LGdA)$_5$/d(DTdC)$_5$. The slope of the fluorescence intensity plot was greater for d(LGdA)$_5$/d(DTdC)$_5$ duplex than that for d(LAdG)$_5$/d(DCdT)$_5$, indicating higher ethidium

Table 2. The Results of Scatchard Analysis

	Association constant per duplex (K)	Association constant per site (k)	Number of intercalation sites (n)
$d(LADG)_5/d(DCDT)_5$	$2.8\times10^6\,M^{-1}$	$1.8\times10^6\,M^{-1}$	1.6 sites
$d(LGDA)_5/d(DTDC)_5$	$5.2\times10^6\,M^{-1}$	$1.2\times10^6\,M^{-1}$	4.4 sites

bromide affinity of the former than the latter. Scatchard plots were derived from the fluorescence data (Table 2). The association constant (k) was calculated from the slope of the plot, and the value for the interaction of ethidium bromide with $d(LADG)_5/d(DCDT)_5$ duplex was $1.8\times10^6\,M^{-1}$, while that with $d(LGDA)_5/d(DTDC)_5$ duplex was $1.2\times10^6\,M^{-1}$. From the intercept of the abscissa, the number of intercalation sites per duplex (n) was estimated to be 4.4 sites/10 bp duplex for $d(LGDA)_5/d(DTDC)_5$, and 1.6 sites/duplex for $d(LADG)_5/d(DCDT)_5$. The results indicate that the association constants of ethidium bromide are almost the same for $d(LADG)_5/d(DCDT)_5$ and $d(LGDA)_5/d(DTDC)_5$. The stronger interaction of ethidium bromide with $d(LGDA)_5/d(DTDC)_5$ is attributed to the higher number of intercalation sites; one molecule of $d(LGDA)_5/d(DTDC)_5$ duplex can accept 4—5 molecules of ethidium bromide, though $d(LADG)_5/d(DCDT)_5$ duplex accepts only 1—2 molecules. Such a difference in the number of intercalation sites should explain the superior enhancement of ethidium fluorescence observed for $d(LGDA)_5/d(DTDC)_5$ in the intercalation study using excess ethidium bromide (Fig. 6).

Discussion

Both $d(LADG)_5$ and $d(LGDA)_5$ interact with their complementary natural DNA, as indicated by UV-mixing curve (Fig. 2) and CD-spectral analysis (Fig. 3). The mode of interaction is pH-dependent; *meso*-$d(Pu)_{10}$/D-$d(Py)_{10}$ forms a duplex at pH 7.5 and a triplex at pH 5.0 (Fig. 2). Such pH-dependent duplex/triplex selectivity also occurs with natural homopurine/homopyrimidine DNAs, and has been explained in terms of the requirement of protonation at the 3-nitrogen of cytosine belonging to the third pyrimidine chain for Hoogsteen base-pair formation.[30-39]

The conformation of *meso*-$d(Pu)_{10}$/D-$d(Py)_{10}$ complex was suggested to be a right-handed helix based on the similarity of the CD spectra of the *meso*/natural complex and the natural right-handed complex (Fig. 4). We observed such a similarity between LD-dA_{12}/D-dT_{12} (*meso*/natural) complex and the corresponding natural complex D-dA_{12}/D-dT_{12}, indicating right-handed helix formation, though LD-dA_{12}/L-dT_{12} (*meso*/enantio) showed an opposite CD spectrum to that of the natural complex (data not shown), indicating a left-handed helix (details will be published elsewhere).

The T_m values show that the *meso*-$d(Pu)_{10}$/D-$d(Py)_{10}$ duplex (T_m=10—12 °C) is less stable than its triplex (T_m=24—34 °C). This explains the monophasic profiles of melting curves even under triplex-forming conditions (Fig. 5). At pH 5.0, the duplex will not be able to retain its hybridized state at the temperature where the third strand has been removed. The T_m values also indicate that the $d(LGDA)_5/d(DTDC)_5$ complex (T_m=10 °C for the duplex and 24 °C for the triplex) is less stable than the $d(LADG)_5/d(DCDT)_5$ complex (T_m=12 °C for the duplex and 34 °C for the triplex). This may suggest that replacement of natural dG in an oligomer with L-dG decreases the affinity to the complementary oligomer with higher efficacy compared to the replacement of natural dA with L-dA, because of the higher stability of the natural G–C base-pair than the natural A–T base-pair. Such lower stability of $d(LGDA)_5/d(DTDC)_5$ complexes is consistent with the smaller hypochromicities shown by $d(LGDA)_5/d(DTDC)_5$ as compared with $d(LADG)_5/d(DCDT)_5$.

meso-$d(Pu)_{10}$/D-$d(Py)_{10}$ duplex binds ethidium bromide and enhances its fluorescence intensity. From the features of the emission spectra of ethidium bromide in the presence of *meso*/natural duplex, the mode of ethidium-DNA interaction is interpreted as intercalation (Fig. 6). The results indicate that ethidium bromide intercalates into a duplex, but not into a triplex, of *meso*-$d(Pu)_{10}$/D-$d(Py)_{10}$ under the conditions used (Fig. 7).[32,40,41] At pH 5.0, the stability of the complex seems to determine the state of the complex, *i.e.*, a triplex or ethidium-intercalated duplex. As a triplex of $d(LADG)_5/d(DCDT)_5$ at pH 5.0 (T_m=32 °C) is more stable than a duplex intercalated with ethidium bromide (T_m=22 °C at pH 7.5), the $d(LADG)_5/d(DCDT)_5$ mixture forms a triplex even in the presence of ethidium bromide. Therefore, addition of $d(LADG)_5/d(DCDT)_5$ to ethidium bromide did not cause apparent enhancement of the fluorescence. (The slight enhancement observed, as well as the slight difference of T_m values of $d(LADG)_5/d(DCDT)_5$ in the presence (32 °C) and the absence (36 °C) of ethidium bromide, might be attributed to the possible existence of ethidium-intercalated duplex in a very small amount.) On the other hand, the ethidium-intercalated duplex of $d(LGDA)_5/d(DTDC)_5$ (T_m=24 °C) is more stable than a triplex (T_m=21 °C). Therefore, we conclude that addition of ethidium bromide to $d(LGDA)_5/d(DTDC)_5$ triplex caused conversion to the ethidium-bound duplex in AM buffer pH 5.0, leading to the enhancement of the fluorescence of ethidium bromide (Table 1). The duplexes are stabilized by ethidium; T_m increases from 11 °C to 22 °C for $d(LADG)_5/d(DCDT)_5$ and from 6 °C to 27 °C for $d(LGDA)_5/d(DTDC)_5$. This is consistent with the enhancement of ethidium fluorescence which was observable at 20 °C but not at 40 °C, and also with the increase of UV-hypochromicity upon addition of ethidium (Fig. 7).

The ethidium fluorescence intensity enhancement by $d(LGDA)_5/d(DTDC)_5$ is stronger than that by $d(LADG)_5/d(DCDT)_5$ in the presence of excess ethidium bromide (Fig. 6). This could be interpreted in terms of the results obtained from Scatchard analysis; the $d(LGDA)_5/d(DTDC)_5$ duplex has more intercalating sites (4—5 sites per 10-mer duplex) than the $d(LADG)_5/d(DCDT)_5$ duplex (1—2 sites per duplex). The association constants are almost the same for $d(LGDA)_5/d(DTDC)_5$ and $d(LADG)_5/d(DCDT)_5$ duplex.

Conclusion

We designed and prepared d(LAdG)$_5$ and d(LGdA)$_5$ as model oligomers of *meso*-d(Pu)$_n$. *Meso*-d(Pu)$_n$ was found to interact with its complementary sequence of natural oligodeoxynucleotide. The interaction showed pH-dependent duplex/triplex selectivity, and the complexes were suggested to have a right-handed helix structure. These characteristics may be common for *meso*-DNAs that have homopurine sequences. Ethidium bromide intercalated into both d(LAdG)$_5$/d(DCdT)$_5$ and d(LGdA)$_5$/d(DTdC)$_5$ duplexes and stabilized them at pH 7.5. On the other hand, at pH 5.0, the d(LAdG)$_5$/2d(DCdT)$_5$ triplex could not bind ethidium, while the d(LGdA)$_5$/2d(DTdC)$_5$ triplex interacted with ethidium and was converted to the ethidium-intercalated duplex. Scatchard analysis showed that the d(LGdA)$_5$/d(DTdC)$_5$ duplex had more intercalation sites than d(LAdG)$_5$/d(DCdT)$_5$, though there was no clear difference in their association constants. Though homopurine oligomers are expected to possess special properties that may not be found in DNAs with random nucleobase sequences, clarification of the nature of *meso*-homopurine oligomer interactions would be helpful in improving our understanding of the molecular recognition chemistry of L-sugar-containing nucleic acids.

Acknowledgment N. I. is very grateful to JSPS Fellowships for Japanese Junior Scientists for financial support.

References

1) Fujimori S., Shudo K., Hashimoto Y., *J. Am. Chem. Soc.*, **112**, 7436—7438 (1990).
2) Tomioka N., Itai A., *Biopolymers*, **32**, 1593—1597 (1992).
3) van Boeckel C. A. A., Visser G. M., Hegstrom R. A., van Boom J. H., *J. Mol. Evol.*, **25**, 100—105 (1987).
4) Tazawa I., Tazawa S., Stempel L. M., Ts'o P. O. P., *Biochemistry*, **9**, 3499—3514 (1970).
5) Ashley G. W., *J. Am. Chem. Soc.*, **114**, 9731—9736 (1992).
6) Kieninger M., Suhai S., *Anticancer Drug Des.*, **10**, 189—201 (1995).
7) Fujimori S., Shudo K., Hashimoto Y., *Nucleic Acids Symp. Ser.*, **22**, 97—98 (1990).
8) Fujimori S., Iwanami N., Shudo K., Hashimoto Y., *Nucleic Acids Symp. Ser.*, **25**, 143—144 (1991).
9) Hashimoto Y., Iwanami N., Fujimori S., Shudo K., *J. Am. Chem. Soc.*, **115**, 9883—9887 (1993).
10) Iwanami N., Shudo K., Hashimoto Y., *Nucleic Acids Symp. Ser.*, **29**, 15—16 (1993).
11) Iwanami N., Fujimori S., Hashimoto Y., Shudo K., *Nucleic Acids Symp. Ser.*, **31**, 45—46 (1994).
12) Asseline U., Hau J.-F., Czernecki S., Diguarher T. L., Perlat M.-C., Valery J.-M., Thuong N. T., *Nucl. Acids Res.*, **19**, 4067—4074 (1991).
13) Damha M. J., Giannaris P. A., Marfey P., Reid L. S., *Tetrahedron Lett.*, **32**, 2573—2576 (1991).
14) Morvan F., Génu C., Rayner B., Gosselin G., Imbach J.-L., *Biochem. Biophys. Res. Commun.*, **172**, 537—543 (1990).
15) Urata H., Ueda Y., Suhara H., Nishioka E., Akagi M., *J. Am. Chem. Soc.*, **115**, 9852—9853 (1993).
16) Garbesi A., Capobianco M. L., Colonna F. P., Tondelli L., Arcamone F., Manzini G., Hilbers C. W., Aelen J. M. E., Blommers M. J. J., *Nucl. Acids Res.*, **21**, 4159—4165 (1993).
17) Blommers M. J. J., Tondelli L., Garbesi A., *Biochemistry*, **33**, 7886—7896 (1994).
18) Damha M. J., Giannaris P. A., Marfey P., *Biochemistry*, **33**, 7877—7885 (1994).
19) Zon G., *Pharm. Res.*, **5**, 539—549 (1988).
20) Miller P. S., Ts'o P. O. P., *Annu. Rep. Med. Chem.*, **23**, 295—304 (1988).
21) Uhlmann E., Peyman A., *Chem. Rev.*, **90**, 543—584 (1990).
22) Thuong N. T., Hélène C., *Angew. Chem. Int. Ed. Engl.*, **32**, 666—690 (1993).
23) Morvan F., Porumb H., Degols G., Lefebvre I., Pompon A., Sproat B. S., Rayner B., Malvy C., Lebleu B., Imbach J.-L., *J. Med. Chem.*, **36**, 280—287 (1993).
24) Milligan J. F., Matteucci M. D., Martin J. C., *J. Med. Chem.*, **36**, 1923—1937 (1993).
25) Fujimori S., Iwanami N., Hashimoto Y., Shudo K., *Nucleosides Nucleotides*, **11**, 341—349 (1992).
26) Sinha N. D., Biernat J., McManus J., Köster H., *Nucl. Acids Res.*, **12**, 4539—4557 (1984).
27) Ti G. S., Gaffney B. L., Jones R. A., *J. Am. Chem. Soc.*, **104**, 1316—1319 (1982).
28) Schaller H., Weimann G., Lerch B., Khorana H. G., *J. Am. Chem. Soc.*, **85**, 3821—3827 (1963).
29) Matteucci M. D., Caruthers M. H., *J. Am. Chem. Soc.*, **103**, 3185—3191 (1981).
30) Rajagopal P., Feigon J., *Biochemistry*, **28**, 7859—7870 (1989).
31) Howard F. B., Frazier J., Lipsett M. N., Miles H. T., *Biochem. Biophys. Res. Commun.*, **17**, 93—102 (1964).
32) Lee J. S., Johnson D. A., Morgan A. R., *Nucl. Acids Res.*, **6**, 3073—3091 (1979).
33) Wells R. D., Collier D. A., Hanvey J. C., Shimizu M., Wohlrab F., *FASEB J.*, **2**, 2939—2949 (1988).
34) Antao V. P., Gray D. M., Ratliff R. L., *Nucl. Acids Res.*, **16**, 719—738 (1988).
35) Rajagopal P., Feigon J., *Nature* (London), **339**, 637—640 (1989).
36) De los Santos C., Rosen M., Patel D., *Biochemistry*, **28**, 7282—7289 (1989).
37) Live D. H., Radhakrishnan I., Misra V., Patel D. J., *J. Am. Chem. Soc.*, **113**, 4687—4688 (1991).
38) Trapane T. L., Ts'o P. O. P., *J. Am. Chem. Soc.*, **116**, 10437—10449 (1994).
39) Singleton S. F., Dervan P. B., *J. Am. Chem. Soc.*, **116**, 10376—10382 (1994).
40) Scaria P. V., Shafer R. H., *J. Biol. Chem.*, **266**, 5417—5423 (1991).
41) Mergny J.-L., Collier D., Rougée M., Montenay-Garestier T., Hélène C., *Nucl. Acids Res.*, **19**, 1521—1526 (1991).